1P5-11

Proceedings of Symposium on Ultrasonic Electronics, Vol. 33 (2012) pp. 113-114
13-15 November, 2012

Increasing Bandwidth of Ultrasound RF Echoes Using Wiener Filter for Speckle Suppression

スペックル抑制のためのウィナーフィルタを用いた超音波 RF エコーの広帯域化

Sho Kageyama[1‡], Hideyuki Hasegawa[1,2] and Hiroshi Kanai[2,1] ([1] Grad. School of Biomed. Eng., Tohoku Univ.; [2] Grad. School of Eng., Tohoku Univ.)
影山　奨 [1†]，長谷川英之 [1,2]，金井　浩 [2,1] ([1] 東北大院　医工, [2] 東北大院　工)

1. Introduction

Ultrasound diagnostic equipment using a pulse-echo method has been widely used in clinical situations. In conventional ultrasound diagnostic equipment, ultrasound images are composed of amplitudes of received ultrasound echoes, and it is known that the image quality is degraded by speckle noise. Therefore, the suppression of speckle noise is an important issue for more accurate diagnosis. In general, a transducer used in ultrasound diagnostic equipment has a narrow-band characteristics. Therefore, the emitted ultrasound pulses show reverberations. Thus, the speckle pattern occurs due to the interference between scattered waves, and a blurred image is obtained. For this reason, for example, thin arterial walls and cancers in very thin bile ducts are difficult to be imaged by conventional ultrasound imaging.

In this report, we have developed a processing method using Wiener filter[1,2] as a technique to broaden the bandwidth of the received signal for suppressing speckle noise. In particular, the transfer function of the transducer and the signal-to-noise ratio (SNR) as a weighting function have been discussed to obtain a desirable filter.

2. Principle

The Wiener filter, which weights to the frequency characteristic of the filter by considering the SNR, is used as a method for speckle noise suppression. The model using a Wiener filter is shown in **Fig. 1**. Frequency spectrum $\hat{F}_{i,j}(\omega)$ of the output signal $\hat{f}_{i,j}(t)$ of the Wiener filter is given by

$$\hat{F}_{i,j}(\omega) = G_{i,j}(\omega) \cdot M_j(\omega) = \frac{G_{i,j}(\omega) \cdot H_j^*(\omega)}{\left|H_j(\omega)\right|^2 + P_N(\omega)/P_F(\omega)}$$

$$= \frac{G_{i,j}(\omega) \cdot \left|H_j(\omega)\right|}{\left|H_j(\omega)\right|^2 + P_N(\omega)/P_F(\omega)} \quad , \qquad (1)$$

where i and j are the beam number and the frame number, respectively. In addition, $G_{i,j}(\omega)$, $H_j(\omega)$, $N(\omega)$, and $M_j(\omega)$ are the frequency spectra of the echo from an object, the

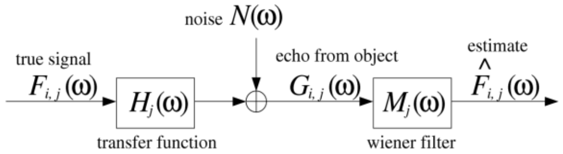

Fig. 1. Wiener filtering model (i: beam position number, j: frame number).

transfer function of the transducer, noise, and the impulse response of the inverse filter, respectively. In eq. (1), $P_N(\omega)$ and $P_F(\omega)$ are the averaged power spectra of noise and estimate $\hat{F}_{i,j}(\omega)$ of the echo from an object, respectively. Wiener filter $M_j(\omega)$ is determined so as to minimize the mean squared difference between the measured signal $g_{i,j}(t)$ and model $\hat{f}_{i,j}(t)$ and is designed using the transfer function $H_j(\omega)$. $H_j(\omega)$ is substituted by the absolute value $|H_j(\omega)|$ in order to avoid the influence of the time delay of the transducer response. Furthermore, determination of the weighting function using the inverse of the SNR included in eq. (1) is essential. It is difficult to use $P_F(\omega)$ in the actual processing since it is the output of the Wiener filter. Therefore, the SNR is determined by the following magnitude-squared coherence function (MSCF)[3] $|\gamma_i(\omega)|^2$.

$$\left|\gamma_i(\omega)\right|^2 = \frac{\left|E_{i,j}\left[G_{i,j}^*(\omega) G_{i,j+1}(\omega)\right]\right|^2}{E_{i,j}\left[\left|G_{i,j}(\omega)\right|^2\right] \cdot E_{i,j}\left[\left|G_{i,j+1}(\omega)\right|^2\right]} \qquad (2)$$

MSCF $|\gamma_i(\omega)|^2$ is a function evaluating the phase coherency of echoes in different frames. Assuming that the signal component has the phase coherency and the noise component is not coherent, SNR is given by

$$\mathrm{SNR} = \frac{1}{N_{\mathrm{beam}}} \sum_{i=0}^{N_{\mathrm{beam}}-1} \frac{\left|\gamma_i(\omega)\right|^2}{1 - \left|\gamma_i(\omega)\right|^2} \quad , \qquad (3)$$

where N_{beam} is the number of beam positions.

As shown in **Fig. 1**, $G_{i,j}(\omega)$ is the frequency spectrum of the echo signal obtained by ultrasound equipment. Assuming that $f_{i,j}(t)$ is the group of impulses, it is considered that $G_{i,j}(\omega)$ is the sum of $\{H_j(\omega)\}$ with different phase characteristics due to time delays of the impulses. In this case, dips occur at particular frequencies in $G_{i,j}(\omega)$ and, therefore, $|G_{i,j}(\omega)|$ is different from $|H_j(\omega)|$. The dips of amplitude spectra randomly occur because of the randomness of scatterer positions. Therefore, the transfer function (transducer response) $|H_j(\omega)|$ is estimated by averaging $\{|G_{i,j}(\omega)|\}$ obtained at different ultrasound beams. $|H_j(\omega)|$ is given by

Email address: kageyama@us.ecei.tohoku.ac.jp
(kanai, hasegawa)@ecei.tohoku.ac.jp

$$|H_j(\omega)| = \frac{1}{N_{\mathrm{beam}}}\sum_{i=0}^{N_{\mathrm{beam}}-1}|G_{i,j}(\omega)| \qquad (4)$$

Figure 2 shows power spectra of echoes from different targets obtained using a 10-MHz linear-type ultrasound probe. Since a fine wire can be assumed as a point scatterer, a dip does not occur as shown in **Fig. 2(c)**. In the case of a glass plate, the ultrasound pulses are almost reflected from the surface of glass. Therefore, the frequency characteristics in all beams are similar as shown in **Fig. 2(b)**. On the other hand, in the case of the silicone plate, there are dips in measured power spectra, as shown in **Fig. 2(a)**, because there are many scatterers inside the silicone plate. Thus, the feasibility of the proposed method was examined using the silicone plate because biological tissue also contains scatterers.

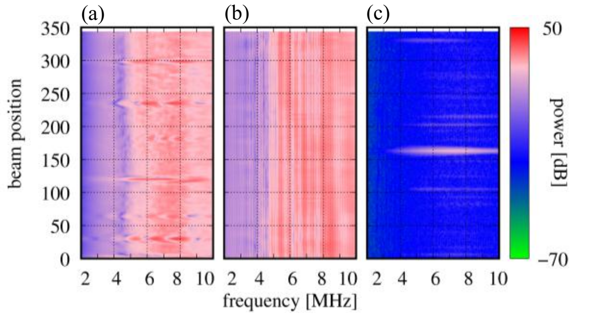

Fig. 2. Power spectra obtained for (a) silicone plate, (b) glass plate, and (c) wire (13 µm in diameter).

Furthermore, both the transfer function $H_j(\omega)$ and the weighting function $P_N(\omega)/P_F(\omega)$ in eq. (1) were normalized to suppress the influence of the reflectivity of the target.

3. Results

As a basic examination, we measured echoes from a silicone plate mimicking ultrasound RF echoes scattered from point scatterers in biological tissue using a 10-MHz linear-type ultrasound probe (equipped to Aloka, SSD-6500) at a sampling frequency of 40 MHz. The number of beams was 344, frame rate was 30, and beam spacing was 0.1 mm. The power spectrum of an echo from the silicone plate $|G_{i,j}(\omega)|^2$ is shown in **Fig. 3**. The bandwidth of $|G_{i,j}(\omega)|^2$ is broadened by applying the Wiener filter.

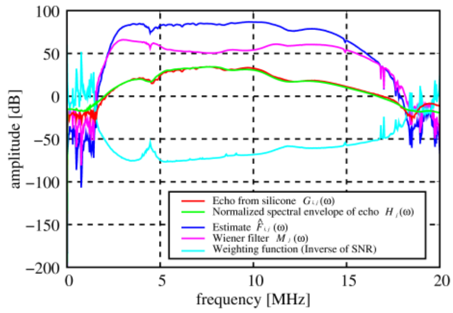

Fig. 3. Power spectra obtained in measurement of the silicone plate (i = 150, j = 0).

Figures 4(a) and (b) show B-mode longitudinal images of a carotid artery. In addition, **Figs. 5(a) and (b)** show RF signal and the envelope of the 126-th beam in the 0-th frame in **Fig. 4**. As shown in **Fig. 5**, T_2 and T_4 show lumen-intima boundary (LIB), T_3 and T_5 show media-adventitia boudary (MAB), T_3-T_2 and T_5-T_4 show intima-media thickness (IMT), and T_4-T_3 shows intravascular lumen. By multiplying the Wiener filter, the difference in the brightnesses between the adventitia and the intima-media complex (IMC) was reduced, and the IMT can be detected more easily. Also, the half width of the echo from the adventitia between T_5 and T_6 obtained by the conventional method is 0.75 mm and that of the proposed estimate is 0.62 mm. The improvement of the spacial resolution by applying the Wiener filter was confirmed.

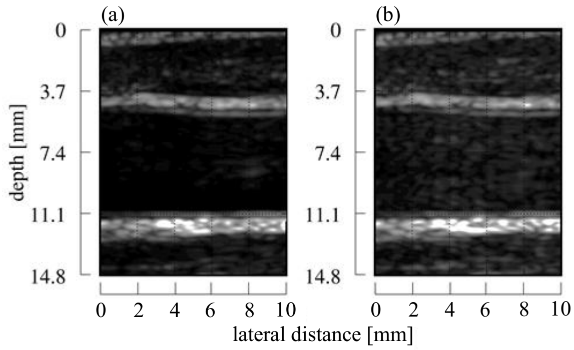

Fig. 4. B-mode longitudinal images of carotid artery. (a) Conventional. (b) With Wiener filter.

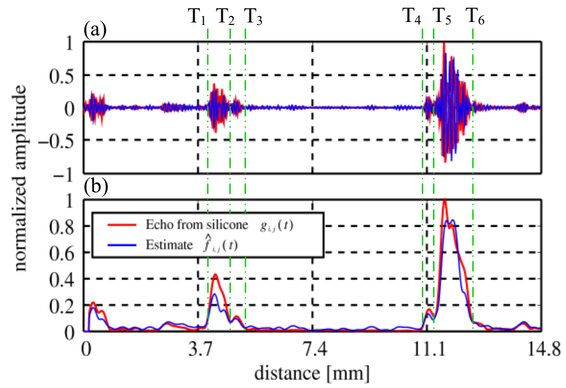

Fig. 5. Echo from silicone and estimate (i = 126, j = 0). (a) RF signal. (b) Envelope.

4. Conclusion

In this study, a method for speckle noise suppression by the Wiener filter was developed using the spatial averaged spectrum of amplitude spectra $\{|G_{i,j}(\omega)|\}$ of received echoes $\{g_{i,j}(t)\}$ from an object as the transducer response $H_j(\omega)$.

References

1. W. K. Pratt: *Digital Image Processing* (John Wiley & Sons, New York, 1978) p. 410.
2. H. C. Andrews and B. R. Hunt: *Digital Image Restoration* (Prentice-Hall, New Jersey, 1997) p. 126.
3. T. Fukushima, H. Hasegawa, H. Kanai: Jpn. J. Appl. Phys. **50** (2011) 07HF02.